Interpretation of polarized Cu K x-ray absorption near-edge-structure spectra of CuO

2001 J. Phys.: Condens. Matter 13 8519

(http://iopscience.iop.org/0953-8984/13/37/309)

INSTITUTE OF PHYSICS PUBLISHING JOURNAL OF PHYSICS: CONDENSED MATTER

J. Phys.: Condens. Matter **13** (2001) 8519–8525 PII: S0953-8984(01)26196-7

Interpretation of polarized Cu K x-ray absorption near-edge-structure spectra of CuO

O Šipr and A Šimůnek

Institute of Physics, Academy of Sciences of the Czech Republic, Cukrovarnická 10, 162 53 Praha 6, Czech Republic

E-mail: sipr@fzu.cz

Received 26 June 2001
Published 30 August 2001
Online at stacks.iop.org/JPhysCM/13/8519

Abstract

Polarized Cu K-edge spectra of CuO are calculated by different methods and compared to experiment. Theoretical spectra were obtained via an all-electron full-potential band-structure calculation based on a pseudopotential technique and by a real-space multiple-scattering method involving a self-consistent muffin-tin potential. Self-consistency in the scattering potential is necessary to describe the low-energy part of the $\varepsilon \parallel z$ partial spectral component. The low-energy shoulder in the $\varepsilon \parallel x$ component observed in the experiment cannot be explained within a one-electron picture and thus apparently has a many-body origin. However, its particular mechanism will be different from the shake-down process suggested for explaining a similar feature in copper–chlorine compounds.

1. Introduction

Copper oxide, CuO, serves as a model for interpreting x-ray absorption near-edge-structure (XANES) spectral features in more complex materials, such as high-T_c superconductors. Therefore, it is clearly desirable to have a well-founded interpretation of its main XANES features. Common understanding of dominant spectral characteristics in the Cu K-edge XANES of CuO has relied mostly on indirect evidence so far. Until recently, theoretical work concentrated rather on related compounds containing $CuCl_2$ or $CuCl_4^{2-}$ molecular complexes [1–3]. Investigations of CuO itself were limited to unpolarized spectra only [4, 5]. This is a severe restriction, as polarized spectra provide a much more stringent test of any interpretation [6].

Recently, Bocharov *et al* [7] undertook a comprehensive study of *polarized* Cu K-edge spectra of CuO, comparing partial spectral components resolved from experimental data with results of a real-space multiple-scattering (RS-MS) calculation for a *non-self-consistent* muffin-tin potential. Despite a good overall agreement, perceptible deficiencies of the theory for

certain energy ranges and/or polarizations were recognized. Such failures could indicate either insufficiency of the non-self-consistent muffin-tin potential or, alternatively, may point to the inability of the one-electron local density approximation (LDA) framework itself to describe certain spectral transitions. Indeed, a many-body origin of some features in the Cu K-edge XANES of CuO was suggested by several authors [8–11], by analogy with [1–3].

In order to get a more definite answer about the origin of the spectral peaks, we compare the experimental polarized Cu K-edge spectra of CuO with several theoretical calculations, involving different approaches and approximations, so that we will be able to separate deficiencies of various one-electron techniques from possible many-body effects. In particular, we employ a full-potential band-structure calculation based on the pseudopotential technique and several RS-MS calculations for muffin-tin potentials constructed in various ways (both self-consistent and non-self-consistent potentials, with a 1s core hole or without it).

2. Methods

Any linearly polarized spectrum can be decomposed into a weighted sum of a few partial spectral components [12]. Polarized experimental spectra of CuO were resolved into three dipole and five quadrupole components [7,13] in a local coordination system, which is depicted in figure 1, and in a global coordination system, which can be attached to crystal axes. We will rely on the local system in this paper, in order to facilitate extending possible implications of our study to the physics of other oxides.

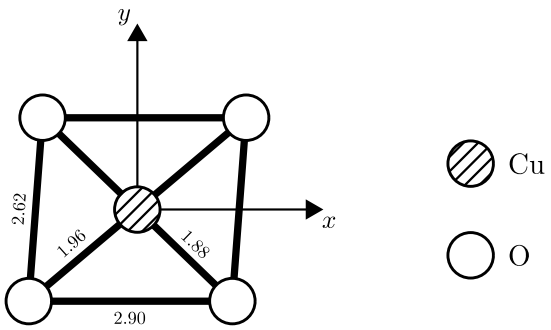

Figure 1. The nearest coordination of a Cu atom in a CuO crystal. A planar CuO_4 complex is shown together with the orientation of the x- and y-axes. The z-axis is perpendicular to the CuO_4 plane. Interatomic distances are in ångströms. (Note that 'slf' stands for 'self-consistent' in the figure labelling.)

The electronic structure of CuO was calculated self-consistently within the LDA by an all-electron method using a pseudopotential formalism and a plane-wave basis set [14]. The technique works with relaxed core states and provides full electron charge densities comparable with results of a full-potential linearized augmented-plane-wave method (see also [15] for a comparison). The Ceperley–Alder exchange and correlation term in an analytical form [16] was used both for occupied and for unoccupied states in our band-structure calculation. To obtain dipole transition matrix elements of the core–valence transition, we split it into its radial and angular parts as follows:

$$\langle \psi_c | \boldsymbol{\varepsilon} \cdot \boldsymbol{r} | \psi_{n\boldsymbol{k}} \rangle = \langle \psi_c | r | \psi_{n\boldsymbol{k}} \rangle_{\mathrm{rad}} \langle \psi_c | \frac{\boldsymbol{\varepsilon} \cdot \boldsymbol{r}}{r} | \psi_{n\boldsymbol{k}} \rangle_{\mathrm{ang}}. \tag{1}$$

In equation (1), $\boldsymbol{\varepsilon}$ is the polarization vector, $\boldsymbol{k}$ is crystal momentum and n is the band subscript. The value of the radial part $\langle \psi_c | r | \psi_{n\boldsymbol{k}} \rangle_{\mathrm{rad}}$ is approximated by a constant in our calculation (this

corresponds to a non-dispersive core state and a single non-dispersive valence state of fixed energy). The angular part was evaluated using the full symmetry and dispersion of the valence wave functions $\psi_{n\boldsymbol{k}}(\boldsymbol{r})$ in the $\boldsymbol{k}$-space and, thus, determines the shape of the spectral peaks. A similar approach for evaluating matrix elements was used in [17].

The RS-MS calculations [18] were performed for a cluster of 189 atoms (cluster size convergency was checked). Three types of muffin-tin potential were used:

(i) a non-self-consistent potential, constructed via superposition of coulombic potentials and charge densities of isolated atoms (Mattheiss prescription [19, 20]);
(ii) a self-consistent potential generated via self-consistent-field (SCF) X_α multiple-scattering molecular calculations [21]; and finally
(iii) a potential constructed from full electron charge densities obtained from self-consistent electronic structure calculations by an all-electron pseudopotential method [14].

In cases (i) and (ii), the influence of the core hole left by the excited electron can be taken into account by moving a 1s electron from the core into the lowest unoccupied atomic or molecular level (relaxed and screened model). Thus, we have five different potentials available for our RS-MS calculations.

For calculating the occupied states, the Ceperley and Alder [16] exchange–correlation potential was employed in atomic calculations for (i) while the X_α-potential with the Kohn–Sham value of $\alpha = 0.66$ [22] was employed in molecular calculations for (ii). In constructing the muffin-tin potential appropriate for unoccupied states, the energy-independent X_α-potential with $\alpha = 0.66$ was employed for all of the RS-MS calculations presented here. We do not employ energy-dependent exchange–correlation potentials as no universal recipe for selecting their optimal form for each particular case is available so far [23–25].

The SCF-X_α molecular calculation for (ii) was done using an adapted XASCF program of Cook and Case [26, 27], using an eleven-atom cluster centred on copper and a nine-atom cluster centred on oxygen. When constructing the intra-cluster muffin-tin-type potential inside the self-consistency loop, these clusters were assumed to be embedded in the infinite CuO crystal. Our approach thus resembles that based on the concept of the local interaction zone [28].

Full electron charge densities obtained from an all-electron full-potential band-structure calculation for (iii) were spherically averaged within spheres around Cu and O sites and a muffin-tin potential was constructed in a standard way thereafter [29].

In principle, self-consistent potentials constructed from charge densities obtained via the SCF-X_α molecular calculation for (ii) and via a band-structure calculation for (iii) can differ: in the first case, the muffin-tin approximation is involved *from the beginning*, thus affecting the self-consistency process itself; while in the second case, the muffin-tin approximation is applied only *after* a full-potential self-consistent band-structure calculation is finished. Significant differences between these two potentials would thus signal a fundamental breakdown of the muffin-tin approximation.

Our band-structure calculation incorrectly resulted in metallic CuO, which is a common deficiency of all LDA calculations [30, 31]. The semiconducting character of CuO can be revealed only in calculations which go beyond the *ab initio* LDA approach [32, 33].

3. Results and discussion

Our results are presented in figure 2. Experimental dipole partial spectral components were taken from [7]. The zero of the energy scale coincides with the Fermi energy of the band-structure calculation; the horizontal alignment between different panels was chosen such that the best overall agreement between dipole peak positions is achieved. All theoretical curves

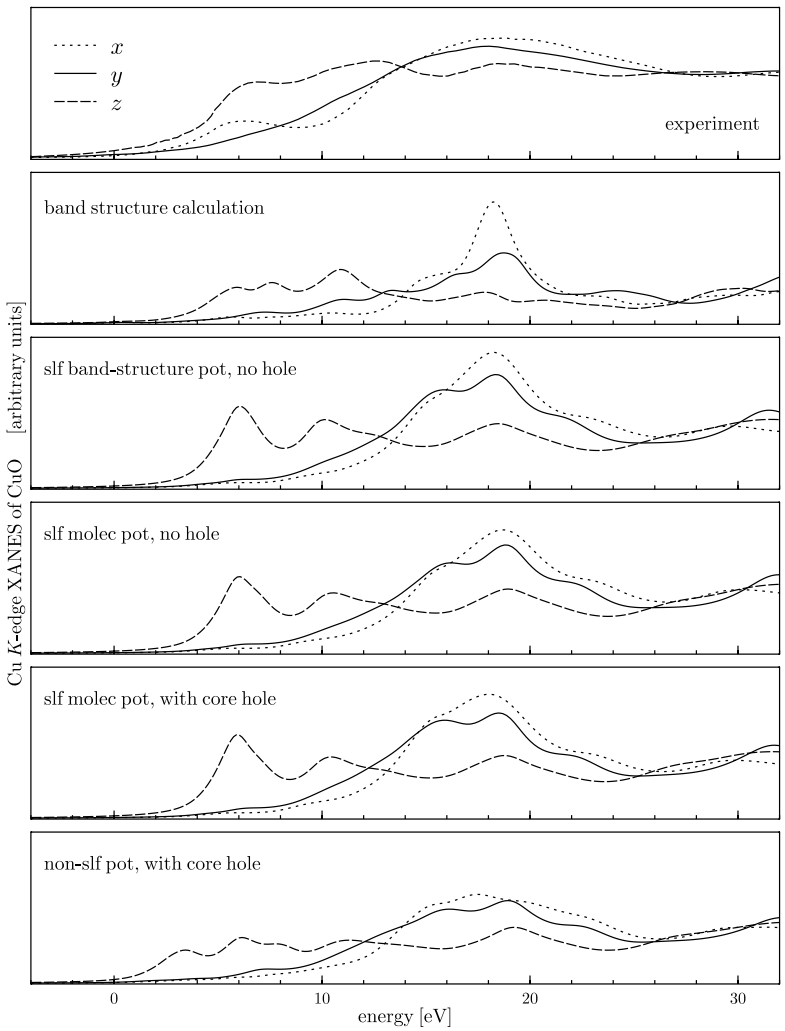

Figure 2. Polarized dipole partial spectral components of Cu K-edge XANES in the local coordinate system. Dotted lines denote $\boldsymbol{\varepsilon} \parallel \boldsymbol{x}$ components, solid lines denote $\boldsymbol{\varepsilon} \parallel \boldsymbol{y}$ components and dashed lines denote $\boldsymbol{\varepsilon} \parallel \boldsymbol{z}$ components. The first panel, from the top, shows the experiment [7, 13]; the panel below it was obtained from band-structure calculation; the third panel corresponds to RS-MS calculation for a muffin-tin potential generated from charge densities borrowed from the band-structure calculation. The fourth and fifth panels show RS-MS calculations for potentials taken from SCF-X_α molecular calculations (either ignoring the core hole or taking it into account) and the lowest panel corresponds to a non-self-consistent potential with a core hole constructed via the Mattheiss prescription.

were convoluted with a Lorentzian function to account for the core-hole lifetime broadening. As the main objective of figure 2 is to facilitate comparison between different theoretical methods, no further broadening was applied, in order to maintain as many spectral details as was reasonably possible.

In general, there is a good agreement between the theoretical curves themselves and between theory and experiment. Some differences appear in the detail; let us deal with them individually.

A non-self-consistent calculation (the lowest panel in figure 2) displays a spurious peak at the very beginning of the spectra—at $E \approx 3$ eV. In principle, there could be several reasons for this failure (lack of self-consistency, non-muffin-tin corrections, many-body effects). We checked that by applying different prescriptions for construction of the muffin-tin potential (leading to different muffin-tin radii and/or muffin-tin zeros), the resulting spectrum changes in detail but the redundant feature itself remains. On the other hand, this peak does not appear in any of the 'self-consistent' panels, no matter whether they involve muffin-tin approximation or not (figure 2). Therefore the *lack of self-consistency* must be the true cause of the occurrence of this false peak.

Hardly any difference can be seen between RS-MS calculations that take the core hole into account and those that ignore it. This is true both for the self-consistent molecular potential and for the non-self-consistent Mattheiss potential as well (we omitted the results corresponding to the Mattheiss potential without a core hole from figure 2 for brevity). It can thus be safely concluded that the (relaxed and screened) core hole has no influence on any of the dipole components of the Cu K-edge spectra of CuO. Application of the band-structure approach, which does not account for the core hole, is thus *a posteriori* justified. The fact that all polarization components behave identically with regard to the core hole is not self-evident, as there are systems where the core-hole effect is actually polarization dependent (see [6]; see also [34]).

The RS-MS calculation presented in the panel third from the top in figure 2 was performed for a muffin-tin potential generated by electron densities taken from the all-electron band-structure calculation, the results for which are presented in the upper panel. Hence, the differences between these two panels may arise either from neglect of energy dependence of the radial part of the matrix element in the band-structure panel (cf. equation (1)), or from neglect of non-muffin-tin effects in the RS-MS panel. As radial parts of matrix elements typically vary only smoothly with the energy [35], one can assume that the largest effect comes from non-muffin-tin effects. The most notable difference between these two calculations occurs for the first $\varepsilon \parallel z$ structure around 6 eV. The double peak in the band-structure panel may—after additional smearing—correspond better to the broad structure seen in the experiment than the relatively sharp peak in the RS-MS case. Also, the ratios of the intensities of the $\varepsilon \parallel z$ peaks at $E \approx 6$ eV and at $E \approx 10$–12 eV are different in the two cases: in the RS-MS curve, the first peak is higher than the second one, while in the band-structure panel, the second peak is higher—in accordance with the experiment. Thus we tentatively suggest that the wrong ratio of the intensities of the $E \approx 6$ eV and $E \approx 10$–12 eV peaks obtained from RS-MS calculations could be a consequence of the muffin-tin approximation. However, as an influence of the energy dependence of the radial parts of the matrix elements cannot be ruled out on this energy scale, this assignment is open to discussion.

The most prominent disagreement between the theory and the experiment in figure 2 consists in the absence of the low-energy shoulder at $E = 6$ eV for the $\varepsilon \parallel x$ polarization in all of our calculations. Due to the variety of techniques involved in obtaining the theoretical curves in figure 2, one can be confident that the source of this failure must lie outside the realm of the one-electron approach. The first explanation of the $E = 6$ eV shoulder that comes to mind is a shake-down process, which was identified as the source of a similar shoulder in copper–chlorine systems [1–3]. However, one ought to apply these results to CuO with some caution: the complexes explored in [1–3] were of planar (or even axial) nature, while the off-plane neighbours of Cu in CuO may play a significant role. Also the polarization dependence of the $E = 6$ eV shoulder is different in CuO to those in the $CuCl_4^{2-}$ complexes: in particular, this shoulder appears only for ε lying in the xy-plane of CuO (figure 2), while it is characteristic for the $\varepsilon \parallel z$ polarization in [1–3].

A shoulder about halfway to the main peak, similar to the one discussed above, appears in XANES spectra of many copper oxides. There is no unanimous opinion as regards its nature. Some authors, relying on the analogy with copper chlorines [1–3], attribute it to shake-down many-body processes [8–11]. Others interpret it within a single-particle picture and support their view with non-self-consistent RS-MS one-electron calculations [36, 37]. It is evident from figure 2 of our paper that the $E = 6$ eV shoulder cannot be reproduced by a one-electron approach. Hence it has to be of many-body origin. Its mechanism, however, will be different to the shake-down mechanism discussed by [1–3], as its polarization dependence is different. In the light of these results, a purely one-electron explanation of the corresponding shoulder in more complex oxides may be worth a second look. In particular, it would be desirable to explore the polarization dependence of the Cu K-edge XANES in the two perpendicular directions in the ab-plane in those compounds. The shoulder peak appears, in fact, in CuO for $\boldsymbol{\varepsilon} \parallel \boldsymbol{x}$ polarization only, while the $\boldsymbol{\varepsilon} \parallel \boldsymbol{y}$ component is basically structureless in that energy region.

A lot of attention has been devoted to the pre-peak in CuO spectra in the past. A comprehensive analysis of its polarization dependence clearly demonstrated its quadrupole nature *by experiment* [7]. We calculated the quadrupole transitions by the same methods as the dipole transitions displayed in figure 2. The agreement with experiment was rather poor in this case: although the quadrupole peaks appear at approximately correct energies, their intensity is far too low with respect to experiment (by at least an order of magnitude). We do not display the calculated quadrupole components here, for brevity. A satisfactory intensity of the quadrupole pre-peak could be obtained only in the case of a non-self-consistent Mattheiss potential with a core hole [7], which seems to be just a fortuitous coincidence given the fact that it cannot be reproduced by RS-MS calculations for self-consistent potentials. We believe that our failure to reproduce the pre-peak quantitatively is a consequence of the failure of the LDA to describe electronic states of CuO in this energy region.

4. Conclusions

By employing two conceptually quite different approaches to XANES calculation, we demonstrated that self-consistency in the scattering potential is necessary for describing the low-energy part of the $\boldsymbol{\varepsilon} \parallel \boldsymbol{z}$ partial spectral component of CuO—otherwise, a spurious peak at $E \approx 3$ eV appears in the calculation. The muffin-tin approximation seems to be quite adequate for description of dipole spectral components for CuO—the only significant deficiency of the muffin-tin constraint could be the inverted ratio of intensities of the peaks at $E \approx 6$ eV and at $E \approx 10$–12 eV for the $\boldsymbol{\varepsilon} \parallel \boldsymbol{z}$ component. A self-consistent calculation demonstrates that the effect of a relaxed core hole in the photoabsorbing atom is negligible for all three polarizations.

The shoulder in the $\boldsymbol{\varepsilon} \parallel \boldsymbol{x}$ component observed in experiment at $E = 6$ eV cannot be explained within a one-electron picture, which indicates its many-body origin. However, the particular mechanism behind it will be different from the shake-down process suggested for explaining a similar feature in copper–chlorine compounds [1–3]. Our analysis of CuO casts doubts on a purely one-electron interpretation of this shoulder feature in the high-T_c oxides Y–Ba–Cu–O and Bi–Sr–Ca–Cu–O and suggests that this could be revealed by analysing spectra polarized along the a- and b-axes separately.

Acknowledgment

This work was supported by project 202/99/0404 of the Grant Agency of the Czech Republic.

References

[1] Bair R A and Goddard W A III 1980 *Phys. Rev.* B **22** 2767
[2] Kosugi N, Yokoyama T, Asakura K and Kuroda H 1984 *Chem. Phys.* **91** 249
[3] Yokoyama T, Kosugi N and Kuroda H 1986 *Chem. Phys.* **103** 101
[4] Norman D, Garg K B and Durham P J 1985 *Solid State Commun.* **56** 895
[5] Šipr O 1992 *J. Phys.: Condens. Matter* **4** 9389
[6] Šipr O, Šimůnek A, Bocharov S, Kirchner Th and Dräger G 1999 *Phys. Rev.* B **60** 14 114
[7] Bocharov S, Kirchner Th, Dräger G, Šipr O, and Šimůnek A 2001 *Phys. Rev.* B **63** 045104
[8] Kosugi N, Tokura Y, Takagi H and Uchida S 1990 *Phys. Rev.* B **41** 131
[9] Choy J H, Kim D K, Hwang S H and Demazeau G 1994 *Phys. Rev.* B **50** 16 631
[10] Liang G, Guo Y, Badresingh D, Xu W, Tang Y, Croft M, Chen J, Sahiner A, Beom-hoan O and Markert J T 1995 *Phys. Rev.* B **51** 1258
[11] Kim M G, Cho H S and Yo Ch H 1998 *J. Phys. Chem. Solids* **59** 1369
[12] Brouder C 1990 *J. Phys.: Condens. Matter* **2** 701
[13] Šipr O, Šimůnek A, Bocharov S, Kirchner Th and Dräger G 2001 *J. Synchrotron Radiat.* **8** 235
[14] Vackář J, Hyt'ha M and Šimůnek A 1998 *Phys. Rev.* B **58** 12 712
[15] Šimůnek A, Vackář J, Polčík M, Drahokoupil J, Wolf W and Podloucky R 2000 *Phys. Rev.* B **61** 4385
[16] See e.g. Pickett W E 1989 *Comput. Phys. Rep.* **9** 115
[17] Šimůnek A, Polčík M and Wiech G 1995 *Phys. Rev.* B **52** 11 865
[18] Vvedensky D D 1992 *Unoccupied Electron States* ed J C Fuggle and J E Inglesfield (Berlin: Springer) p 139
[19] Mattheiss L F 1964 *Phys. Rev.* **133** A1399
Mattheiss L F 1964 *Phys. Rev.* **134** A970
[20] Loucks T L 1967 *Augmented Plane Wave Method* (New York: Benjamin)
[21] Johnsson K H 1973 *Adv. Quantum Chem.* **7** 143
[22] Kohn W and Sham L J 1965 *Phys. Rev.* **140** A1133
[23] Chaboy J and Quartieri S 1995 *Phys. Rev.* B **52** 6349
[24] Ankudinov A L and Rehr J J 1997 *J. Physique Coll.* IV **7** C2 121
[25] Ankudinov A L 1999 *J. Synchrotron Radiat.* **6** 236
[26] Cook M and Case D A 1980 *Computer Code XASCF* Quantum Chemistry Program Exchange, Indiana University, Bloomington, IN
[27] Šipr O, Rocca F and Dalba G 1999 *J. Synchrotron Radiat.* **6** 770
[28] Nicholson D M C, Stocks G M, Wang Y, Shelton W A, Szotek Z and Temmerman W M 1994 *Phys. Rev.* B **50** 14 686
[29] Moruzzi V, Janak J and Williams A 1984 *Calculated Electronic Properties of Metals* (New York: Pergamon)
[30] Ching W Y, Xu Y-N and Wong K W 1989 *Phys. Rev.* B **40** 7684
[31] Mariot J-M, Barnole V, Hague C F, Vetter G and Queyroux F 1989 *Z. Phys.* B **75** 1
[32] Anisimov V I, Zaanen J and Andersen O K 1991 *Phys. Rev.* B **44** 943
[33] Takahashi M and Igarashi J 1997 *Phys. Rev.* B **56** 12 818
[34] Tolentino H, Medarde M, Fontaine A, Baudelet F, Dartyge E, Guay D and Tourillon G 1992 *Phys. Rev.* B **45** 8091
[35] Müller J E and Wilkins J W 1984 *Phys. Rev.* B **29** 4331
[36] Bianconi A, Li C, Campanella F, Della Longa S, Pettiti I, Pompa M, Turtù S and Udron D 1991 *Phys. Rev.* B **44** 4560
[37] Li C, Pompa M, Congiu Castellano A, Della Longa S and Bianconi A 1991 *Physica* C **175** 369